Approximation-Free Control for Nonlinear Helicopters With Unknown Dynamics

Shubo Wang, *Member, IEEE*

***Abstract*—This brief presents an approximation-free control scheme for nonlinear helicopter systems with unknown dynamics. Without using the function approximation methods (e.g., neural network (NN) or fuzzy logic system (FLS)), the developed approximation free controller has a simple proportional-like structure, which can reduce the computational complexity, thus suitable for practical applications. Finally, comparative simulations are provided to show the effectiveness and superior performance of the proposed control scheme.**

***Index Terms*—Approximation-free control, prescribed performance control, robust control, helicopters.**

I. Introduction

THE CONTROL of nonlinear helicopters has been widely investigated due to their potential applications in military and civilian areas. In helicopter control systems, the unknown dynamics such as system uncertainties and external disturbances may deteriorate the control performance. To handle the unknown dynamics, many control schemes have been developed such as PID and linear quadratic regulator (LQR) [1]. However, these control methods can not achieve satisfactory control performance. Recently, with rapid development of control techniques, various advanced control strategies have been proposed for helicopters to improve the control performance, e.g., optimal control [2], robust control [3], adaptive control [4]–[8], etc. Moreover, the intelligent control technologies (e.g., neural network (NN) [9], [10] or fuzzy logic system (FLS) [11], [12]) have also been utilized to control complex nonlinear systems owing to their approximation abilities. Although satisfactory control performance have been obtained, the transient and state-steady performance are difficult to establish in the control design.

To tackle this issue, a new control strategy named prescribed performance control (PPC) was developed in [13], [14]. The main idea is that an original controlled system was transformed into a new control system by utilizing a prescribed performance function (PPF), and then the new error system was used to design controllers [15]–[20]. Nevertheless, in all aforementioned control approaches with PPF, function approximators were corporated into the control design to deal with the unknown system dynamics so that the computational burden may be increased. Recently, an approximation free control scheme was developed [14] to control the nonlinear system which can reduce the computational burdens. However, this approach has not yet been investigated for the nonlinear 3-DOF helicopters.

In this brief, we will study the approximation free control for 3-DOF helicopters with unknown dynamics. One salient feature is that the proposed control scheme can guarantee the output performance specifications, regarding convergence rate, overshoot, and state-steady performance. Compared with backstepping control methods, the proposed control scheme has a simpler proportional-like structure and by not using filtering operation completely avoids the explosion phenomenon. These benefits of the proposed control scheme will be verified by the simulation results based on a 3-DOF helicopter. The main contributions of this brief are summarized as follows: (i) An approximation-free control scheme is developed for the nonlinear helicopters, where function approximations are not used even in the presence of the unknown dynamics. (ii)The developed control can not only achieve reduced computational burdens but also improve the transient and state-steady performance.

Manuscript received December 20, 2021; accepted January 9, 2022. Date of publication January 12, 2022; date of current version June 29, 2022. This work was supported in part by the National Natural Science Foundation of China under Grant 62173194, and in part by the National Natural Science Foundation of Shandong Province under Grant ZR2021YQ41. This brief was recommended by Associate Editor J. Wu.

The author is with the School of Automation and the Shandong Key Laboratory of Industrial Control Technology, Qingdao University, Qingdao 266071, China (e-mail: wangshubo1130@126.com).

Color versions of one or more figures in this article are available at https://doi.org/10.1109/TCSII.2022.3142426.

Digital Object Identifier 10.1109/TCSII.2022.3142426

II. Preliminaries

Consider the following initial value problem

$$\dot{\mu}(t) = \psi(t, \mu), \quad \mu(0) = \mu^0 \in \Omega_\mu \tag{1}$$

where $\psi : R_+ \times \Omega_\mu \to R^n$ denotes a continuous function, and $\Omega_\mu \in R^n$ represents a non-empty set.

Lemma 1 [14]: For the equation (1), if function $\psi(t, \mu)$ satisfies the following conditions: i) the function $\psi(t, \mu)$ is locally Lipschitz for $t > 0$, and ii) piecewise continuous and locally integrable on t for $\mu(t) \in \Omega_\mu$, there is a solution $\mu(t)$ on $[0, \rho_{max})$ with $\rho_{max} > 0$.

Proposition 1 [14]: For a maximal solution $\mu(t)$ on the interval $[0, \rho_{max})$ with $\rho_{max} < \infty$ for any compact set $\bar{\Omega}_\mu \in \Omega_\mu$, there is a time constant $t_1 \in [0, \rho_{max})$ such that $\mu(t) \notin \bar{\Omega}_\mu$.

III. Problem Formulation

A. System Dynamic Model

The nonlinear 3-DOF helicopter systems can be described as

$$\begin{aligned} J_a\ddot{\varepsilon} &= L_a \cos p u_1 - g(M_h L_a - M_w L_w)\cos\varepsilon + F_\varepsilon \\ J_b\ddot{p} &= L_h u_2 + F_p \end{aligned} \tag{2}$$

1549-7747 © 2022 IEEE. Personal use is permitted, but republication/redistribution requires IEEE permission.
See https://www.ieee.org/publications/rights/index.html for more information.

Authorized licensed use limited to: Keio University. Downloaded on April 09,2023 at 07:00:04 UTC from IEEE Xplore. Restrictions apply.

TABLE I
SYSTEM PARAMETERS

Parameters	Units	definition
ε	rad	Elevation angle
p	rad	Pitch angle
λ	rad	Travel angle
J_ε	kg $\cdot m^2$	Inertia of elevation axis
J_p	kg $\cdot m^2$	Inertia of pitch axis
J_λ	kg $\cdot m^2$	Inertia of travel axis
u_f	V	Front motor voltage input
u_b	V	Back motor voltage input
K_f	N/V	Propeller force-thrust constant
g	m/s^{-2}	Gravity acceleration
M_h	Kg	Mass of helicopter
M_w	Kg	Mass of counterweight
L_a	m	Distance from travel axis to helicopter body
L_w	m	Distance from travel axis to counterweight
L_h	m	Distance between the pitch and each motor

where $\begin{bmatrix} u_1 \\ u_2 \end{bmatrix} = \begin{bmatrix} K_f(u_f + u_b) \\ K_f(u_f - u_b) \end{bmatrix}$, and F_ε and F_p denote the model uncertainties and unknown disturbances. The system parameters are shown in Table I.

Assumption 1: The model uncertainties and unknown disturbances F_ε and F_p are bounded.

Define the state variables as $x = [x_1, x_2, x_3, x_4]^T = [\varepsilon, \dot{\varepsilon}, p, \dot{p}]^T$, the state-space equation can be expressed as

$$\begin{aligned} \dot{x}_1 &= x_2 \\ \dot{x}_2 &= \frac{L_a}{J_a}\cos x_3 u_1 - \frac{g}{J_a}(M_h L_a - M_w L_w)\cos x_1 + F_\varepsilon \\ \dot{x}_3 &= x_4, \quad \dot{x}_4 = \frac{L_h}{J_b}u_2 + F_p. \end{aligned} \tag{3}$$

B. Prescribed Performance Control

To study the transient performance of the helicopters, the prescribed performance function is defined as

$$\varphi(t) = (\varphi_0 - \varphi_\infty)e^{-at} + \varphi_\infty \tag{4}$$

with $0 < \varphi_\infty < \varphi_0, \quad a > 0$, where φ_0, φ_∞, and a are design parameters.

According to [21], the errors $e(t)$ should satisfy the following inequality:

$$-\underline{\delta}\varphi(t) < e(t) < \bar{\delta}\varphi(t) \tag{5}$$

where $\underline{\delta}$ and $\bar{\delta}$ denote the upper and lower bounds, respectively.

Introducing a function $\Lambda(z)$, which has the following properties:1. $-\delta < \Lambda(z) < \delta, \quad \forall z \in L_\infty$; 2. $\lim_{z\to-\infty}\Lambda(z) = -\delta$, and $\lim_{z\to\infty}\Lambda(z) = \delta$.

Then, the tracking error is given as

$$e(t) = \varphi(t)\Lambda(z) \tag{6}$$

Thus, the inverse function of $\Lambda(z)$ can be described as

$$z(t) = \Lambda^{-1}\left[\frac{e(t)}{\varphi(t)}\right] \tag{7}$$

The function $\Lambda(z)$ is expressed as

$$\Lambda(z) = \frac{\bar{\delta}e^{z(t)} - \underline{\delta}e^{-z(t)}}{e^{z(t)} + e^{-z(t)}} \tag{8}$$

The new error $z(t)$ is defined as

$$z(t) = \frac{1}{2}\ln\frac{\mu(t) + \underline{\delta}}{\bar{\delta} - \mu(t)} \tag{9}$$

where $\mu(t) = e(t)/\varphi(t)$.

From (9), we can conclude that for any initial tracking error $e(0)$, if parameters φ_0, φ_∞, and a are chosen such that $-\underline{\delta}\varphi(0) < e(0) < \bar{\delta}\varphi(0)$ and $z(t)$ can be controlled to be bounded, then $-\delta < \Lambda(z) < \delta$ holds.

IV. APPROXIMATION-FREE CONTROL DESIGN

A. Control Design

In this section, the design steps are given as follows.

Step I 1: Define the tracking error as $e_1 = x_1 - y_\varepsilon$, where y_ε is the target signal. Based on (9), the transformed error is

$$z_1(t) = \Lambda^{-1}(\mu_1(t)) \tag{10}$$

where $\mu_1(t) = e_1(t)/\varphi_1(t)$, and $\varphi_1(t)$ is defined as

$$\varphi_1(t) = (\varphi_{10} - \varphi_{1\infty})e^{-a_1 t} + \varphi_{1\infty} \tag{11}$$

where φ_{10}, $\varphi_{1\infty}$ and a_1 are the positive constants, and the $e_1(0)$ should satisfy $|e_1(0)| < \min\{\underline{\delta}, \bar{\delta}\}\varphi_{10}$. The intermediate controller can be designed as

$$\vartheta_1 = -k_1 z_1 = -\frac{k_1}{2}\ln\left(\frac{\underline{\delta} + \mu_1}{\bar{\delta} - \mu_1}\right) \tag{12}$$

where $k_1 > 0$ is positive constant.

Step I 2: Define the intermediate controller error as $e_2 = x_2 - \vartheta_1$. The second transformed error is given as

$$z_2(t) = \Lambda^{-1}(\mu_2(t)) \tag{13}$$

where $\mu_2(t) = e_2(t)/\varphi_2(t)$, and $\varphi_2(t)$ is defined as

$$\varphi_2(t) = (\varphi_{20} - \varphi_{2\infty})e^{-a_2 t} + \varphi_{2\infty} \tag{14}$$

where φ_{20}, $\varphi_{2\infty}$ and a_2 are the positive constants, and the $e_2(0)$ should satisfy $|e_2(0)| < \min\{\underline{\delta}, \bar{\delta}\}\varphi_{20}$. Then, the second intermediate controller is designed as

$$u_1 = -k_2 z_2 = -\frac{k_2}{2}\ln\left(\frac{\underline{\delta} + \mu_2}{\bar{\delta} - \mu_2}\right) \tag{15}$$

where $k_2 > 0$ denotes a constant.

Step II 1: Define the tracking error as $e_3 = x_3 - y_p$, where y_p is the target signal. Based on (9), the transformed error is

$$z_3(t) = \Lambda^{-1}(\mu_3(t)) \tag{16}$$

where $\mu_3(t) = e_3(t)/\varphi_3(t)$, and $\varphi_3(t)$ is defined as

$$\varphi_3(t) = (\varphi_{30} - \varphi_{3\infty})e^{-a_3 t} + \varphi_{3\infty} \tag{17}$$

where φ_{30}, $\varphi_{3\infty}$ and a_3 are the positive constants, and the $e_3(0)$ should satisfy $|e_3(0)| < \min\{\underline{\delta}, \bar{\delta}\}\varphi_{30}$. The intermediate controller can be designed as

$$\vartheta_3 = -k_3 z_3 = -\frac{k_3}{2}\ln\left(\frac{\underline{\delta} + \mu_3}{\bar{\delta} - \mu_3}\right) \tag{18}$$

where $k_3 > 0$ is positive constant.

Authorized licensed use limited to: Keio University. Downloaded on April 09,2023 at 07:00:04 UTC from IEEE Xplore. Restrictions apply.

Step II 2: Define the intermediate controller error as $e_4 = x_4 - \vartheta_3$. The second transformed error is

$$z_4(t) = \Lambda^{-1}(\mu_4(t)) \tag{19}$$

where $\mu_4(t) = e_4(t)/\varphi_4(t)$, and $\varphi_4(t)$ is defined as

$$\varphi_4(t) = (\varphi_{40} - \varphi_{4\infty})e^{-a_4 t} + \varphi_{4\infty} \tag{20}$$

where φ_{40}, $\varphi_{4\infty}$ and a_4 are the positive constants, and the $e_4(0)$ should satisfy $|e_4(0)| < \min\{\underline{\delta}, \bar{\delta}\}\varphi_{40}$. Then, the second intermediate controller is designed as

$$u_2 = -k_4 z_4 = -\frac{k_4}{2}\ln\left(\frac{\underline{\delta} + \mu_4}{\bar{\delta} - \mu_4}\right) \tag{21}$$

where $k_4 > 0$ denotes a constant.

B. Stability Analysis

Theorem 1: For 3-DOF helicopter systems described by (2), we proposed the intermediate controllers (12), (18), and actual control laws (15) and (21) with PPF. If the error e_i fills the initial conditions $|e_i(0)| < \min\{\underline{\delta}, \bar{\delta}\}\varphi_{i0}$, then the tracking error e_1 can be guaranteed within the prescribed boundary and all the signals are bounded.

Proof: Based on the intermediate controller errors and its associated normalized error $\mu_i(t)$, the state variables are defined as:

$$\begin{aligned} x_1 &= \varphi_1\mu_1 + y_\varepsilon, \quad x_2 = \varphi_2\mu_2 + \vartheta_1 \\ x_3 &= \varphi_3\mu_3 + y_p, \quad x_4 = \varphi_4\mu_4 + \vartheta_3 \end{aligned} \tag{22}$$

By substituting (22) into (4), the time derivatives of $\mu_i, i = 1, \ldots, 4$ can be written as

$$\begin{aligned} \dot{\mu}_1 &= \frac{1}{\varphi_1}\big[(\dot{x}_1 - \dot{y}_\varepsilon) - \mu_1\dot{\varphi}_1\big] = \frac{1}{\varphi_1}\big[\varphi_2\mu_2 + \vartheta_1 - \dot{y}_\varepsilon - \mu_1\dot{\varphi}_1\big] \\ &= \psi_1(t, \mu_1, \mu_2) \\ \dot{\mu}_2 &= \frac{1}{\varphi_2}\Big[(\dot{\hat{\vartheta}}_2 - \dot{\vartheta}_1) - \mu_2\dot{\varphi}_2\Big] \\ &= \frac{1}{\varphi_2}\Big[\frac{L_a}{J_a}\cos x_3 u_1 - \frac{g}{J_a}(M_h L_a - M_w L_w)\cos x_1 + F_\varepsilon \\ &\quad - \dot{\vartheta}_1 - \mu_2\dot{\varphi}_2\Big] = \psi_2(t, \mu_2, \mu_3) \\ \dot{\mu}_3 &= \frac{1}{\varphi_3}\Big[(\dot{\hat{\vartheta}}_3 - \dot{y}_p) - \mu_3\dot{\varphi}_3\Big] \\ &= \frac{1}{\varphi_3}\big[(\varphi_4\mu_4 + \vartheta_3 - \dot{y}_p) - \mu_3\dot{\varphi}_3\big] = \psi_3(t, \mu_3, \mu_4) \\ \dot{\mu}_4 &= \frac{1}{\varphi_4}\big[(\dot{x}_4 - \dot{\vartheta}_3) - \mu_4\dot{\varphi}_4\big] \\ &= \frac{1}{\varphi_4}\Big[\frac{L_h}{J_b}u_2 + F_p - \dot{\vartheta}_3) - \mu_4\dot{\varphi}_3\Big] = \psi_4(t, \mu_3, \mu_4) \end{aligned} \tag{23}$$

By defining the error vector $\mu = [\psi_1, \psi_2, \psi_3, \psi_4]^T$, then (23) be written as

$$\dot{\mu} = \psi(t, \mu) = \begin{bmatrix} \psi_1(t, \mu_1, \mu_2) \\ \psi_2(t, \mu_2, \mu_3) \\ \psi_3(t, \mu_3, \mu_4) \\ \psi_4(t, \mu_3, \mu_4) \end{bmatrix} \tag{24}$$

In this sequel, the proof of Theorem 1 will be conducted in two phases. First, the existence and uniqueness of a maximal solution over a set Ω_μ is ensured. Second, we will prove that the boundedness of all closed loop signals for all $t \in [0, \rho_{max})$, which leads by contradiction to $\rho_{max} = +\infty$.

Phase A: The PPF $\varphi_i,\ i = 1, \ldots, 4$ have been selected to satisfy $\varphi_i(0) > \min\{\underline{\delta}, \bar{\delta}\}|e_i(0)|$. As a consequence $|\mu_i(0)| < \min\{\underline{\delta}, \bar{\delta}\}$, which results in $\mu_i(0) \in \Omega_\mu$. Furthermore, the function $\psi_i(t)$ is bounded and piecewise continuous on t as well as locally Lipschitz on μ over the set Ω_μ since the reference signal x_d and performance function φ_i are bounded and continuous differentiable and virtual controller ϑ_i and actual controller u are smooth over the set Ω_μ. Therefore, the conditions in Theorem holds and the existence of a maximal solution $\mu : [0, \rho_{max}) \to \Omega_\mu$ of (24) on a time interval $[0, \rho_{max})$ is ensured.

Phase B: This phase proves the boundedness of all closed loop signals for $t \in [0, \rho_{max})$. Differentiating z_1, applying $\dot{x}_1 = x_2 = \varphi_2\mu_2 + \vartheta_1$ in (22), we obtain

$$\dot{z}_1 = \tfrac{\partial\Lambda^{-1}}{\partial\mu_1}\dot{\mu}_1 = \rho_1(\varphi_2\mu_2 + \vartheta_1 - \mu_1\dot{\varphi}_1) \tag{25}$$

where $\rho_1 = 1/(2\varphi_1)[1/(\mu_1 + \underline{\delta}) - 1/(\mu_1 - \bar{\delta})]$ is a positive constant, and fulfills $0 < \rho \le \rho_{M1}$.

By applying similar mathematical manipulations as (25) for z_2, z_3, and z_4, one can further obtain:

$$\begin{aligned} \dot{z}_2 &= \frac{\partial\Lambda^{-1}}{\partial\mu_2}\dot{\mu}_2 = \rho_2\big[(\dot{x}_2 - \dot{\vartheta}_1) - \mu_2\dot{\varphi}_2\big] \\ &= \rho_2\Big[\frac{L_a}{J_a}\cos x_3 u_1 - \frac{g}{J_a}(M_h L_a - M_w L_w)\cos x_1 \\ &\qquad + F_\varepsilon - \dot{\vartheta}_1 - \mu_2\dot{\varphi}_2\Big] \\ \dot{z}_3 &= \frac{\partial\Lambda^{-1}}{\partial\mu_3}\dot{\mu}_3 = \rho_3\big[(\dot{x}_3 - \dot{\vartheta}_2) - \mu_3\dot{\varphi}_2\big] \\ &= \rho_3\big[(\varphi_4\mu_4 + \vartheta_3 - \dot{\vartheta}_2) - \mu_3\dot{\varphi}_2\big] \\ \dot{z}_4 &= \frac{\partial\Lambda^{-1}}{\partial\mu_3}\dot{\mu}_3 = \rho_4\big[(\dot{x}_4 - \dot{\vartheta}_3) - \mu_4\dot{\varphi}_3\big] \\ &= \rho_4\Big[\frac{L_h}{J_b}u_2 + F_p - \dot{\vartheta}_3 - \mu_4\dot{\varphi}_4\Big] \end{aligned} \tag{26}$$

where $\rho_i = 1/(2\varphi_i)[1/(\mu_i + \underline{\delta}) - 1/(\mu_i - \bar{\delta})]$ is positive constant, and fulfills $0 < \rho_i \le \rho_{Mi}, i = 2, 3, 4$.

Step 1: Select a Lyapunov function as

$$V_1 = \frac{1}{2}z_1^2 \tag{27}$$

The time derivative of V_1 along (25) as

$$\dot{V}_1 = z_1\dot{z}_1 = z_1\rho_1(\mu_2\varphi_2 - \mu_1\dot{\varphi}_1 - k_1 z_1) \tag{28}$$

Because $\dot{\varphi}_1$ and φ_2 are bounded, and $|\mu_i(t)| < \min\{\underline{\delta}, \bar{\delta}\}$. According to the extreme value theorem, we have

$$|\mu_2\varphi_2 - \mu_1\dot{\varphi}_1| \le \varpi_1 \tag{29}$$

where ϖ_1 is a positive constant. One has

$$\dot{V}_1 \le |z_1|\rho_{M1}(\varpi_1 - k_1|z_1|) \tag{30}$$

From (30), we can conclude that $\dot{V}_1$ is negative for any $|z_1| > \varpi_1/k_1$. According to the Lyapunov theorem, z_1 can converge to a compact set $\Psi_1 := \{z_1 | |z_1| \le z_{M1}\}$ with

Authorized licensed use limited to: Keio University. Downloaded on April 09,2023 at 07:00:04 UTC from IEEE Xplore. Restrictions apply.

$z_{M1} = \max\{|z_1(0)|, \varpi_1/k_1\}$ for $\forall t \in [0, \rho_{max})$. Thus, we can conclude that the control signal ϑ_1 and $\dot{z}_1$ are bounded. Therefore, the tracking error e_1 can be guaranteed within a prescribed bounded.

Step 2: Consider a Lyapunov function as

$$V_2 = \frac{1}{2}z_2^2 \tag{31}$$

The time derivative of V_2 can be obtained along (26)

$$\begin{aligned}\dot{V}_2 &= z_2\rho_2\bigg[\frac{L_a}{J_a}\cos x_3 u_1 - \frac{g}{J_a}(M_hL_a - M_wL_w)\cos x_1 \\ &\qquad + F_\varepsilon - \dot{\vartheta}_1 - \mu_2\dot{\varphi}_2\bigg] \\ &\le |z_2|\rho_{M2}\big[\varpi_2 - k_2|z_2|L_a/J_a\cos x_3 + F_\varepsilon\big]\end{aligned} \tag{32}$$

where $|k_f(-\frac{g}{J_a}(M_hL_a - M_wL_w)\cos x_1 - \dot{\vartheta}_1 - \mu_2\dot{\varphi}_2| \le \varpi_2$, $\forall t \in [0, \rho_{max})$ is a positive constant. Because $|z_2(t)| < \min\{\underline{\delta}, \bar{\delta}\}$, and μ_2, $\dot{\mu}_2$, μ_1, and $\dot{\vartheta}_1$ are bounded, thus ϖ_2 can be verified. Then, we can claim that z_2 will converge to a compact set $\Psi_2 := \{z_2 | |z_2| \le z_{M2}\}$ with $z_{M2} = \max\{|z_2(0)|, J_a(\varpi_2 + F_\varepsilon)/(k_2L_a\cos x_1)\}$. Therefore, the controller u_1 is also bounded, and the error e_2 is remained within a prescribed bounded.

Step 3: Similarly, a Lyapunov function is selected as $V_3 = z_3^2/2$, and the time derivative of V_3 is

$$\dot{V}_3 = z_3\rho_3[\mu_3\varphi_3 - k_3z_3 - \mu_2\dot{\varphi}_2] \le |z_3|\rho_{M3}(\varpi_3 - k_3|z_3|) \tag{33}$$

where $\varpi_3 > 0$ is a positive constant, which denote the upper bound $|\mu_3\varphi_3 - \mu_2\dot{\varphi}_2| \le \varpi_3$, $\forall t \in [0, \rho_{max})$. Because $|z_3(t)| < \min\{\underline{\delta}, \bar{\delta}\}$, and μ_3, $\dot{\mu}_3$, μ_2 and $\dot{\vartheta}_2$ are bounded, we can claim that z_3 can converge to $\Psi_3 := \{z_3 | |z_3| \le z_{M3}\}$ with $z_{M3} = \{z_3(0)|, \varpi_3/k_3\}$ for $\forall t \in [0, \rho_{max})$. Therefore, the intermediate controller ϑ_3 and its derivative $\dot{\vartheta}_3$ are also bounded. Based on Lemma 1, the tracking error e_3 remains within a predefined bounded.

Step 4: Choose a Lyapunov function $V_4 = z_4^2/2$, the time derivative of V_4 is

$$\begin{aligned}\dot{V}_4 &= z_4\rho_4\bigg[\frac{L_h}{J_b}u_2 + F_p - \dot{\vartheta}_3 - \mu_4\dot{\varphi}_4\bigg] \\ &\le |z_4|\rho_{M4}\big[\varpi_4 - k_4|z_4|L_h/J_b + F_p\big]\end{aligned} \tag{34}$$

where $\varpi_4 > 0$ is a positive constant, which presents the upper bound of $|-\dot{\vartheta}_3 - \mu_4\dot{\varphi}_4| \le \varpi_4$, $\forall t \in [0, \rho_{max})$. Because μ_4, $\dot{\mu}_4$, μ_3 and $\dot{\vartheta}_3$ are bounded, we can conclude that z_4 can converge to a compact set $\Psi_4 := \{z_4 | |z_4| \le z_{M4}\}$ with $z_{M4} = \max\{|z_4(0)|, J_b(\varpi_4 + F_b)/(L_hk_4)\}$. Therefore, the control law u and control error e_4 are also bounded for $t \in [0, \rho_{max})$.

In the follows, we need to show that $\rho_{max} = \infty$. Notice that $z(t) \in \bar{\Omega}_u$, $\forall t \in [0, \rho_{max})$, where the set $\bar{\Omega} = [\underline{\delta}, \bar{\delta}] \times [\underline{\delta}, \bar{\delta}] \times [\underline{\delta}, \bar{\delta}] \times [\underline{\delta}, \bar{\delta}]$ is nonempty and compact. Clearly, it can be verified that $\bar{\Omega}_\mu \subset \Omega_\mu$. Hence, we assume $\rho_{max} < +\infty$, the Proposition 1 indicates that there exists a time constant $t' \in [0, \rho_{max})$ such that $z(t') \notin \bar{\Omega}_\mu$, which is a clear contradiction. Therefore, we conclude that $\rho_{max} = \infty$. Consequently, we can prove that all the signals of the closed-loop system are bounded. This completes the proof. ■

Remark 1: Compared to the backstepping method, the design controllers (12), (15), (18) and (21) are proportional-like controls with the $\mu_i(t)$ and the transformation error $z_i = \Lambda^{-1}(\mu_i(t))$. Therefore, the developed control approach is simpler than backstepping procedure. Another salient feature of the proposed control is that no a priori knowledge of the system nonlinearities or their upper bounds is required. Moreover, the function approxiamtions (NN or FLS) are avoided in the control design so that the potentially sluggish online learning can be remedied.

V. Simulations

This section will employ the Quanser 3-DOF helicopter model to show the numerical simulations. The detailed Quanser 3-DOF helicopter parameters are given as $u_f = u_b[0, 12]$V, $K_f = 0.85$N/V, $g = 9.8m/s^{-2}$, $M_h = 1.87$Kg, $M_w = 2.21$Kg, $L_a = 0.545$m, and $L_w = 0.444$m. The parameter uncertainties and unknown disturbances are $F_\varepsilon = 0.05\sin(t)$ and $F_\varepsilon = 0.1$.

To show the control performance, the following three control schemes are compared.

(1) *Approximation Free Control (AFC):* According to the proposed controller in Section IV, the control parameters are selected as $k_1 = 10$, $k_2 = 100$, $k_3 = 11$ and $k_4 = 80$. The PPF parameters are chosen as $\varphi_{10} = \varphi_{20} = \varphi_{30} = \varphi_{40} = 0.1$, $\varphi_{1\infty} = \varphi_{2\infty} = \varphi_{3\infty} = \varphi_{4\infty} = 0.001$, $\bar{\delta} = 1.2$, $\bar{\delta} = 1.2$, and $a_i = 1.2$.

(2) *PID:* The PID controller is designed as $u = -K_pz - K_i\int zdt - K_d\dot{z}$, where $z = [e_1, e_3]^T$ is the tracking error, and K_p, K_i and K_d denote the control gains, which can be defined as $K_p = [5\ 0;\ 0\ 5]^T$, $K_i = [0.2\ 0;\ 0\ 0.2]^T$, and $K_d = [12\ 0;\ 0\ 12]^T$.

(3) *Backstepping Control (BC):* This method is the conventional backstepping control method, the controller gains are the same as AFC.

Case 1:—To validate the control performance, the sinusoidal signals are employed as the desired trajectories for yaw axis and pitch axis $y_\varepsilon = 10 \cdot \frac{\pi}{180}\sin(0.3\pi t - \pi/2)$ and $y_p = 15 \cdot \frac{\pi}{180}\sin(0.2\pi t)$. Comparative control performance is depicted in Fig. 1, it is seen that the design AFC can guarantee the tracking error within a predefined boundary, while the tracking errors of BC and PID approaches exceed the prescribed boundary. This is mainly because the design AFC contains the PPF, and thus improve the transient response and state-steady performance. Moreover, among all these controllers, PID control gives the larger error.

Case 2:—To further validate the control performance, the square wave signals $y_\varepsilon = 10$ with period $T = 50$ and $y_p = 20$ with period $T = 75$ are adopted. As shown in Fig. 2, the proposed AFC can achieve the satisfactory control performance. The tracking error of AFC is smaller than BC and PID. In these three controllers, PID produces the worst control performance. From all the results, one can conclude that compared with BC and PID, the proposed AFC method can guarantee the tracking error in both transient and state-steady performance.

Authorized licensed use limited to: Keio University. Downloaded on April 09,2023 at 07:00:04 UTC from IEEE Xplore. Restrictions apply.

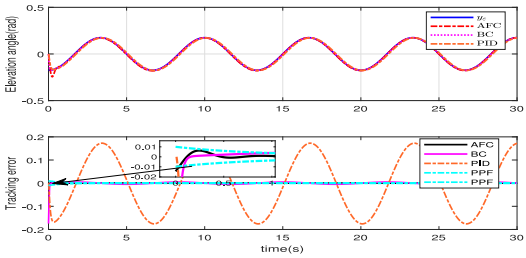

(a)

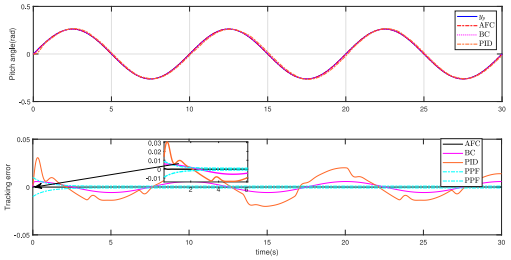

(b)

Fig. 1. Simulation results: (a) Elevation, and (b) Pitch.

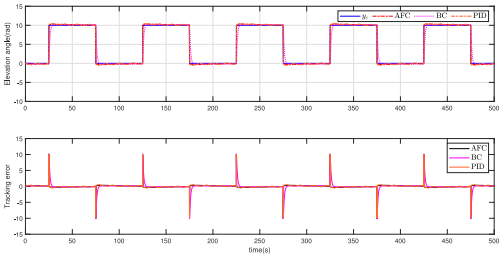

(a)

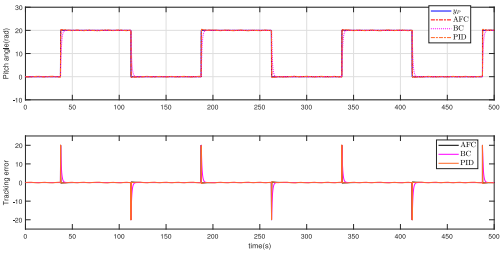

(b)

Fig. 2. Simulation results: (a) Elevation, and (b) Pitch.

VI. Conclusion

This brief presented an approximation free control scheme for nonlinear helicopter systems with unknown dynamics, without using the conventional function approximation methods. To improve the tracking control performance, a PPF with maximum overshoot, steady-state error, and convergence rate is used in the control design. Moreover, the explosion of complexity problem in the traditional backstepping control approaches is overcome without using filtering operation. Finally, the comparative simulation results have demonstrated the effectiveness of proposed control scheme. In the future work, we will focus on solving the singularity problem in approximation free control.

References

[1] H. Liu, G. Lu, and Y. Zhong, "Robust LQR attitude control of a 3-DOF laboratory helicopter for aggressive maneuvers," *IEEE Trans. Ind. Electron.*, vol. 60, no. 10, pp. 4627–4636, Oct. 2013.

[2] B. Luo, H. Wu, and T. Huang, "Optimal output regulation for model-free quanser helicopter with multistep Q-learning," *IEEE Trans. Ind. Electron.*, vol. 65, no. 6, pp. 4953–4961, Jun. 2018.

[3] B. Zheng and Y. Zhong, "Robust attitude regulation of a 3-DOF helicopter benchmark: Theory and experiments," *IEEE Trans. Ind. Electron.*, vol. 58, no. 2, pp. 660–670, Feb. 2011.

[4] Y. Li, S. Tong, L. Liu, and G. Feng, "Adaptive output-feedback control design with prescribed performance for switched nonlinear systems," *Automatica*, vol. 80, pp. 225–231, Jun. 2017.

[5] Y. Ouyang, L. Dong, L. Xue, and C. Sun, "Adaptive control based on neural networks for an uncertain 2-DOF helicopter system with input deadzone and output constraints," *IEEE/CAA J. Automatica Sinica*, vol. 6, no. 3, pp. 807–815, May 2019.

[6] H. Yang, B. Jiang, H. H. T. Liu, H. Yang, and Q. Zhang, "Attitude synchronization for multiple 3-DOF helicopters with actuator faults," *IEEE/ASME Trans. Mechatronics*, vol. 24, no. 2, pp. 597–608, Apr. 2019.

[7] W. He, X. Mu, L. Zhang, and Y. Zou, "Modeling and trajectory tracking control for flapping-wing micro aerial vehicles," *IEEE/CAA J. Automatica Sinica*, vol. 8, no. 1, pp. 148–156, Jan. 2021.

[8] X. Yang and X. Zheng, "Adaptive NN backstepping control design for a 3-DOF helicopter: Theory and experiments," *IEEE Trans. Ind. Electron.*, vol. 67, no. 5, pp. 3967–3979, May 2020.

[9] Y. Li, Y. Liu, and S. Tong, "Observer-based neuro-adaptive optimized control of strict-feedback nonlinear systems with state constraints," *IEEE Trans. Neural Netw. Learn. Syst.*, early access, Jan. 26, 2021, doi: 10.1109/TNNLS.2021.3051030.

[10] B. Fan, Q. Yang, X. Tang, and Y. Sun, "Robust ADP design for continuous-time nonlinear systems with output constraints," *IEEE Trans. Neural Netw. Learn. Syst.*, vol. 29, no. 6, pp. 2127–2138, Jun. 2018.

[11] P. Du, Y. Pan, H. Li, and H. Lam, "Nonsingular finite-time event-triggered fuzzy control for large-scale nonlinear systems," *IEEE Trans. Fuzzy Syst.*, vol. 29, no. 8, pp. 2088–2099, Aug. 2021.

[12] X. Yu, W. He, H. Li, and J. Sun, "Adaptive fuzzy full-state and output-feedback control for uncertain robots with output constraint," *IEEE Trans. Syst., Man, Cybern., Syst.*, vol. 51, no. 11, pp. 6994–7007, Nov. 2021.

[13] C. P. Bechlioulis and G. A. Rovithakis, "Adaptive control with guaranteed transient and steady state tracking error bounds for strict feedback systems," *Automatica*, vol. 45, no. 2, pp. 532–538, 2009.

[14] C. P. Bechlioulis and G. A. Rovithakis, "A low-complexity global approximation-free control scheme with prescribed performance for unknown pure feedback systems," *Automatica*, vol. 50, no. 4, pp. 1217–1226, 2014.

[15] Z. Li, X. Zhang, C. Su, and T. Chai, "Nonlinear control of systems preceded by preisach hysteresis description: A prescribed adaptive control approach," *IEEE Trans. Control Syst. Technol.*, vol. 24, no. 2, pp. 451–460, Mar. 2016.

[16] L. Zhang and G. Yang, "Adaptive fuzzy prescribed performance control of nonlinear systems with hysteretic actuator nonlinearity and faults," *IEEE Trans. Syst., Man, Cybern., Syst.*, vol. 48, no. 12, pp. 2349–2358, Dec. 2018.

[17] Y. Zhu, J. Qiao, and L. Guo, "Adaptive sliding mode disturbance observer-based composite control with prescribed performance of space manipulators for target capturing," *IEEE Trans. Ind. Electron.*, vol. 66, no. 3, pp. 1973–1983, Mar. 2019.

[18] W. Meng, Q. Yang, Y. Ying, Y. Sun, Z. Yang, and Y. Sun, "Adaptive power capture control of variable-speed wind energy conversion systems with guaranteed transient and steady-state performance," *IEEE Trans. Energy Convers.*, vol. 28, no. 3, pp. 716–725, Sep. 2013.

[19] Y. Liu and H. Chen, "Adaptive sliding mode control for uncertain active suspension systems with prescribed performance," *IEEE Trans. Syst., Man, Cybern., Syst.*, vol. 51, no. 10, pp. 6414–6422, Oct. 2021.

[20] S. Wang, H. Yu, J. Yu, J. Na, and X. Ren, "Neural-network-based adaptive funnel control for servo mechanisms with unknown dead-zone," *IEEE Trans. Cybern.*, vol. 50, no. 4, pp. 1383–1394, Apr. 2020.

[21] C. P. Bechlioulis and G. A. Rovithakis, "Robust adaptive control of feedback linearizable MIMO nonlinear systems with prescribed performance," *IEEE Trans. Autom. Control*, vol. 53, no. 9, pp. 2090–2099, Oct. 2008.

Authorized licensed use limited to: Keio University. Downloaded on April 09,2023 at 07:00:04 UTC from IEEE Xplore. Restrictions apply.